Physics Letters B 747 (2015) 193–199

Contents lists available at ScienceDirect

Physics Letters B

www.elsevier.com/locate/physletb

Probing gauge-phobic heavy Higgs bosons at high energy hadron colliders

Yu-Ping Kuang [a,b,*], Ling-Hao Xia [a]

[a] Department of Physics, Tsinghua University, Beijing, 100084, China
[b] Center for High Energy Physics, Tsinghua University, Beijing, 100084, China

ARTICLE INFO

Article history:
Received 19 March 2015
Received in revised form 28 May 2015
Accepted 28 May 2015
Available online 3 June 2015
Editor: G.F. Giudice

ABSTRACT

We study the probe of the gauge-phobic (or nearly gauge-phobic) heavy Higgs bosons (GPHB) at high energy hadron colliders including the 14 TeV LHC and the 50 TeV Super Proton–Proton Collider (SppC). We take the process $pp \to t\bar{t}t\bar{t}$, and study it at the hadron level including simulating the jet formation and top quark tagging (with jet substructure). We show that, for a GPHB with $M_H < 800$ GeV, M_H can be determined by adjusting the value of M_H in the theoretical $p_T(b_1)$ distribution to fit the observed $p_T(b_1)$ distribution, and the resonance peak can be seen at the SppC for $M_H = 800$ GeV and 1 TeV.

1. Introduction

The most important event in the 7 and 8 TeV runs of the LHC is the discovery of the 125 GeV Higgs boson [1,2]. The ATLAS and CMS Collaborations have been making efforts to measure its couplings to the gauge bosons, $\tau^+\tau^-$, and $b\bar{b}$ [3–5], and the obtained results are all consistent with the corresponding standard model (SM) couplings to the present experimental precision. However, this does not imply that the SM is the final theory of fundamental interactions since the SM with a 125 GeV Higgs boson suffers from various shortcomings, such as the well-known theoretical problems [6–8]; the facts that it does not include the dark matter; it can neither predict the mass of the Higgs boson nor predict the masses of all the fermions, etc. Searching for new physics beyond the SM is the most important goal of future particle physics studies. So far there is no evidence of some well-known new physics models such as supersymmetry, large extra dimensions, etc. We know that most known new physics models contain more than one Higgs bosons in which the lightest one may be very close to the SM Higgs boson, and the masses of other heavy Higgs bosons are usually of the order of 10^2–10^3 GeV. So that the discovered 125 GeV Higgs boson may be the lightest Higgs boson in certain new physics model, and probing other heavy Higgs bosons may be a feasible way of searching for new physics. Heavy Higgs bosons in the minimal supersymmetric extension of the SM (MSSM) and the two-Higgs-doublet model (2HDM) have been searched for at the LHC with negative results [9]. So that performing a model-independent search is more effective.

In our previous paper [10], we proposed a sensitive way of probing anomalous heavy neutral Higgs bosons H model-independently at the 14 TeV LHC via the process $pp \to VH^* \to VVV \to \ell^+\nu_\ell j_1 j_2 j_3 j_4$, where $V = W, Z$. We showed that the resonance peak of H and the values of the anomalous coupling constants f_W, f_{WW} can be measured experimentally provided the HVV couplings are not so small. Of course, this cannot be applied to gauge-phobic (or nearly gauge-phobic) heavy Higgs bosons (GPHB) with vanishing (or very small) HVV couplings. For a GPHB H with mass M_H in the 400 GeV to a few TeV range, its main decay mode is $H \to t\bar{t}$. If we simply consider the $t\bar{t}$ final state, the background will be extremely large. Ref. [11] showed that the process $pp \to t\bar{t}H \to t\bar{t}t\bar{t}$ is a feasible process, and studied it at the parton level in the 2HDM. In this paper, we take the process $pp \to t\bar{t}t\bar{t}$, and study the full tree level contribution at the hadron level including simulating the jet formation and top quark tagging (with jet substructure). We show that, with suitable kinematic cuts, the GPHB mass M_H can be determined by adjusting the value of M_H in the theoretical $p_T(b_1)$ distribution to fit the experimentally measured $p_T(b_1)$ distribution for $M_H < 800$ GeV at both the LHC and the 50 TeV Super Proton–Proton Collider (SppC) considered in Beijing, and the resonance peak can be seen at the SppC for $M_H = 800$ GeV and 1 TeV.

* Corresponding author at: Department of Physics, Tsinghua University, Beijing, 100084, China.
E-mail addresses: ypkuang@mail.tsinghua.edu.cn (Y.-P. Kuang), xlh10@mails.tsinghua.edu.cn (L.-H. Xia).

http://dx.doi.org/10.1016/j.physletb.2015.05.073

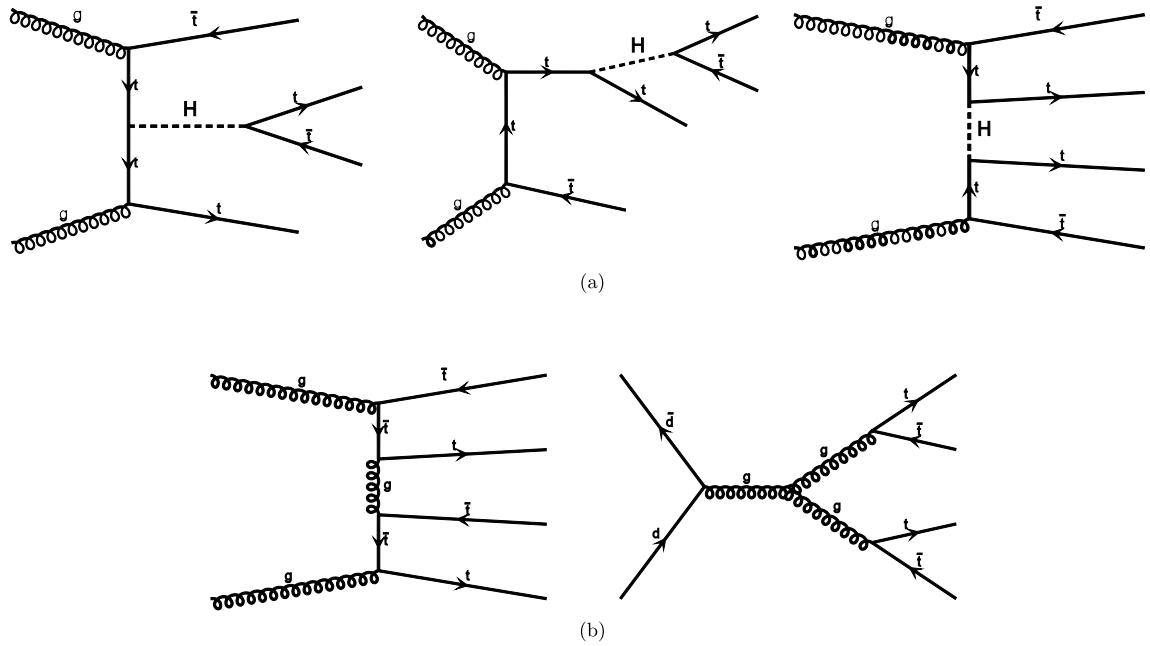

Fig. 1. Some typical Feynman diagrams in $pp \to t\bar{t}t\bar{t}$: (a) for S, and (b) for IB.

Table 1
Detector acceptance according to DELPHES3.

	μ	e	jet	photon
$\|\eta\|_{max}$	2.4	2.5	5	2.5
p_{Tmax} (GeV)	10	10	20	0.5

2. Calculation and results

The general Yukawa coupling of the GPHB with the top quark can be written as

$$y_t^H \bar{t}\Phi_H t \equiv C_t y_t^{SM} \bar{t}\Phi_H t, \tag{1}$$

where C_t is a parameter reflecting the deviation from the SM coupling. For simplicity, we take $C_t \approx 1$. In this paper, we take $M_H = 400$ GeV, 600 GeV, 800 GeV, and 1 TeV as examples to do the calculation.

Ref. [12] shows that the next-to-leading-order correction to the four-top production cross section in the SM is not so large. So we do the leading full tree level simulation of $pp \to t\bar{t}t\bar{t}$ at hadron colliders in this paper. We use MadGraph5 [13], FeynRules [14] and Pythia6.4 [16] to simulate the signals and the backgrounds. We take CTEQ6.1 [15] as the parton distribution function (PDF). Delphes3 [17] and fastjet [18] are used to simulate detector acceptance and jet reconstruction. Our detector acceptance is shown in Table 1 referring to the design of CMS detector [19].

Some typical Feynman diagrams for the signal (S) and the irreducible background (IB) in $pp \to t\bar{t}t\bar{t}$ are depicted in Fig. 1. These two amplitudes will interfere with each other, so that they should be calculated together.

To suppress the SM background, we need some of the decay modes of the top quarks to include leptons. The CMS Collaboration has studied the production of $t\bar{t}t\bar{t}$ in the SM with the final state including a single lepton and multiple jets at the 8 TeV LHC [20], and has shown that it suffers from a very strong SM background. The ATLAS Collaboration analyzed the production of $t\bar{t}t\bar{t}$, and pointed out that, with the energy and integrated luminosity of the LHC Run I, the most favorable final state is the one with two same-sign leptons [21]. Processes with fewer final state leptons can have larger cross sections but with lower signal to background ratios. In this paper, we shall present our simulation results for two kinds of final states. First we study the final states including three charged leptons (3-lepton mode) in which the SM reducible backgrounds (RBs) are highly suppressed. Next we study the final states including two opposite-sign leptons (2-lepton mode) in which the resonance peak of H can be observed.

2.1. The case of 3-lepton mode

We first study the case of 3-lepton mode, i.e. three of the four top (anti-top) quarks in the final state decay semileptonically while the other top (anti-top) quark decays hadronically. A signal event must contain $2\ell^+1\ell^-$ or $1\ell^+2\ell^-$ (ℓ denotes μ or e), and at least three tagged b jets. For reducible backgrounds (RB), there are three most important processes which can mimic the signal:

- **RB1: $\ell^+\ell^- b\bar{b}t\bar{t}$**

Processes with $\ell^+\ell^-$, $b\bar{b}$, and $t\bar{t}$ in the final state. One t (or $\bar{t}$) decays semileptonically and the other $\bar{t}$ (or t) decays hadronically (cf. Fig. 2(a)).

- **RB2: $t\bar{t}t$ + jets and $t\bar{t}\bar{t}$ + jets**

Processes with $t\bar{t}$ and another single top (anti-top) quark with extra jets in the final state. All the three top (anti-top) quarks decay semileptonically. We take one of the extra jets generated by matrix element and the other jets generated by parton shower (cf. Fig. 2(b)).

- **RB3: $\ell^+\ell^- b\bar{b}t$ + jets and $\ell^+\ell^- b\bar{b}\bar{t}$ + jets**

Processes with $\ell^+\ell^-$, $b\bar{b}$, and a top (anti-top) quark with extra jets in the final state. The top (anti-top) quark decays semileptonically. We take one of the extra jets generated by matrix element and the other jets generated by parton shower (cf. Fig. 2(c)).

We generate events for S + IB, IB and RBs at the 14 TeV LHC and the 50 TeV SppC, and do the detector simulation with Delphes3 [17]. Anti-k_T algorithm with $R = 0.5$ are used to cluster jets and tag b jets. For the b-tagging efficiencies, we use the values in Ref. [22]. Then we apply the following kinematic cut: Requiring the event to contain three leptons ($2\ell^+1\ell^-$ or $2\ell^-1\ell^+$) and at least three tagged b jets, i.e.

$$N(\ell^\pm) = 2,\ N(\ell^\mp) = 1,\ \ N(b) \geq 3. \tag{2}$$

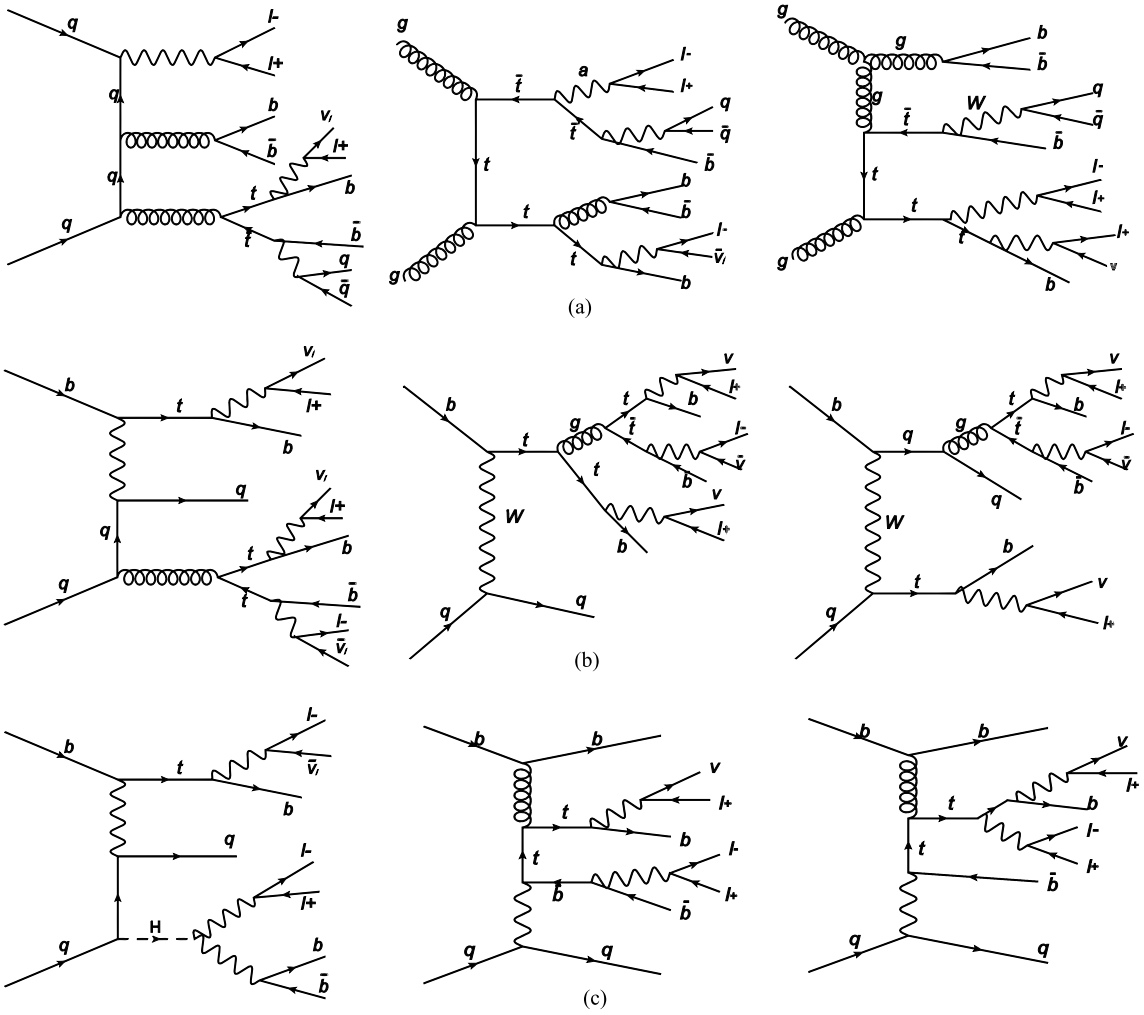

Fig. 2. Feynman diagrams for typical RBs in the case of 3-lepton mode.

Table 2
Cross sections (in fb) of S + IB, IB and RBs for various values of M_H after the cut in case of 3-lepton mode.

	S + IB				IB	RB1	RB2	RB3
	400 GeV	600 GeV	800 GeV	1000 GeV				
14 TeV LHC	0.14	0.10	0.079	0.066	0.060	1.3×10^{-6}	1.3×10^{-9}	6.4×10^{-7}
50 TeV SppC	3.87	3.31	2.63	2.21	1.92	0.039	0.00032	0.0039

Since the S and the IB cross sections cannot be exactly separated, we define the IB, S, and total-background (B) cross section by $\sigma_{\rm IB} \equiv \sigma_{\rm S+IB}(C_t = 0)$, $\sigma_{\rm S} \equiv \sigma_{\rm S+IB}(C_t \neq 0) - \sigma_{\rm IB}$ [23], and $\sigma_{\rm B} \equiv \sigma_{\rm IB} + \sigma_{\rm RB}$, respectively. Here $\sigma_{\rm B}$ is the total SM background.

After this cut, the cross sections of S + IB, IB and RBs for various values of M_H are shown in Table 2. We see that RBs are negligibly small after the cut, and a smaller M_H leads to larger signal cross section. Since the RBs are already negligible, we do not need to impose the top quark tagging requirement taking account of the jet substructure.

For an integrated luminosity $\mathsf{L}_{\rm int}$, the signal and background event numbers are $N_{\rm S} = \mathsf{L}_{\rm int}\sigma_{\rm S}$ and $N_{\rm B} = \mathsf{L}_{\rm int}\sigma_{\rm B}$, respectively. For large enough $N_{\rm S}$ and $N_{\rm B}$, the statistical significance is defined as $\sigma_{\rm stat} = N_{\rm S}/\sqrt{N_{\rm B}}$. The $\mathsf{L}_{\rm int}$ needed for 1σ, 3σ, and 5σ deviations at the 14 TeV LHC and the 50 TeV SppC are shown in Table 3. We see that the 5σ case for $M_H = 600$ GeV, and the 3σ and 5σ cases for $M_H \geq 800$ GeV at the LHC require very high luminosities which need the upgraded high luminosity LHC. All other cases can be reached at the present 14 TeV LHC and the SppC.

Table 3
Integrated luminosity (in fb^{-1}) needed for 1σ, 3σ and 5σ deviations at the 14 TeV LHC and the 50 TeV SppC for different values of M_H.

		400 GeV	600 GeV	800 GeV	1000 GeV
14 TeV LHC	1σ	10	37	172	1664
	3σ	87	341	1552	14977
	5σ	241	947	4312	41604
50 TeV SppC	1σ	0.52	1.0	3.8	23
	3σ	4.6	9.1	34	205
	5σ	13	25	96	570

Since there are three missing neutrinos in the case of 3-lepton mode, it is hard to construct the invariant mass distribution of the top quark pair from the decay of H to show the resonance peak of H. However, the values of M_H may affect the distribution of

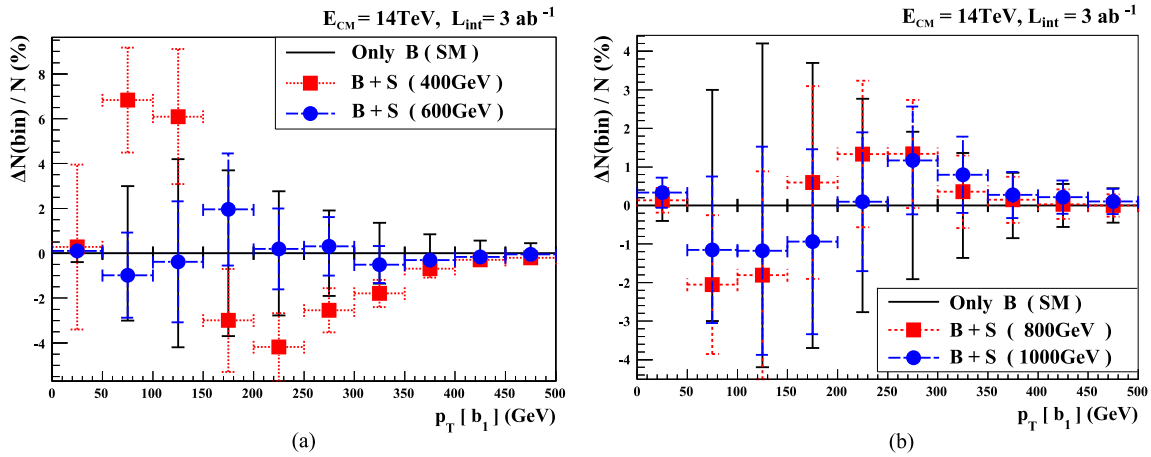

Fig. 3. $\Delta N_{S+B}(\text{bin})/N_{S+B} - \Delta N_B(\text{bin})/N_B$ with statistical errors at 14 TeV LHC: (a) $M_H = 400$ and 600 GeV, (b) $M_H = 800$ and 1000 GeV.

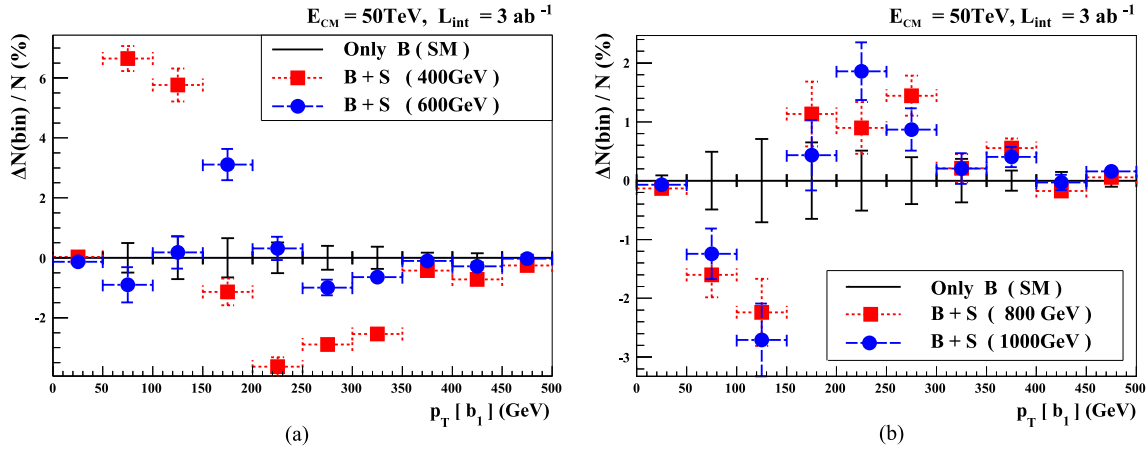

Fig. 4. $\Delta N_{S+B}(\text{bin})/N_{S+B} - \Delta N_B(\text{bin})/N_B$ with statistical errors at 50 TeV SppC: (a) $M_H = 400$ and 600 GeV, (b) $M_H = 800$ and 1000 GeV.

certain kinematic observable from which we may determine the value of M_H. In the final state, the b ($\bar{b}$) quark is the secondary decay product which is more closely related to H than the charged leptons and ordinary jets (from W decays) do. Let b_1 be the b quark with largest p_T. We choose the $p_T(b_1)$ distribution to reflect the effects of different values of M_H. Note that the unknown value of C_t also affects the $p_T(b_1)$ distribution as an overall factor. To eliminate this effect, we separate the $p_T(b_1)$ axis into a certain number of bins. Let $\Delta N(\text{bin})$ be the number of events within a bin at a certain value of $p_T(b_1)$, and $N \equiv \sum_{\text{bin}} \Delta N(\text{bin})$ be the total number of events in the $p_T(b_1)$ distribution. We then take the *normalized* distribution (ND), $\Delta N(\text{bin})/N$, for both S + B (in which the unknown C_t dependence is cancelled) and B (SM background). In Figs. 3 and 4, we plot the ND, $\Delta N_{S+B}(\text{bin})/N_{S+B} - \Delta N_B(\text{bin})/N_B$, with statistical errors for various values of M_H with an integrated luminosity of 3 ab^{-1} at the 14 TeV LHC and the 50 TeV SppC, respectively.

We see that the distributions are clearly distinguishable for $M_H < 800$ GeV at the LHC (the distributions for $M_H > 800$ GeV can hardly be distinguished at the 14 TeV LHC), and they are distinguishable for all values of M_H at the 50 TeV SppC. Thus the value of M_H can be determined by adjusting the value of M_H in the theoretical $p_T(b_1)$ distribution to fit the experimentally measured $p_T(b_1)$ distribution.

Furthermore, if we adjust the value of C_t in σ_{S+B} to fit the observed cross section, we may also determine the value of C_t for the GPHB in nature. Of course the uncertainty depends on the experimental error.

2.2. The case of 2-lepton mode

To be able to show the H resonance peak, we consider the case of 2-lepton mode with the top quark pair from H decay decaying hadronically. When a top (anti-top) quark is highly boosted, its decay products can be clustered into a single fat jet by a clustering algorithm with a large R. And we can tag such a top (anti-top) quark at a high efficiency using jet substructure methods which are reviewed in papers [24,25].

Some typical Feynman diagrams for S and IB before top quark decay are shown in Fig. 1. A signal event must contains two opposite-sign leptons, two tagged b jets, and two tagged t jets. The most important RBs which mimic the signal are:

- **RB-1: $t\bar{t}jj$**

Processes with a $t\bar{t}$ pair and two extra jets in the final state. The $t\bar{t}$ pair decay semileptonically (cf. Fig. 5(a)).

- **RB-2: $\ell^+\ell^- b\bar{b}jj$**

Processes with a $\ell^+\ell^-$ pair, a $b\bar{b}$ pair and two extra jets in the final state (cf. Fig. 5(c)). In **RB-1** and **RB-2**, we only generate two large-p_T jets in the matrix element simulation in order to simplify the calculation. A fully merged background may modify the results, but the modification will not be significant.

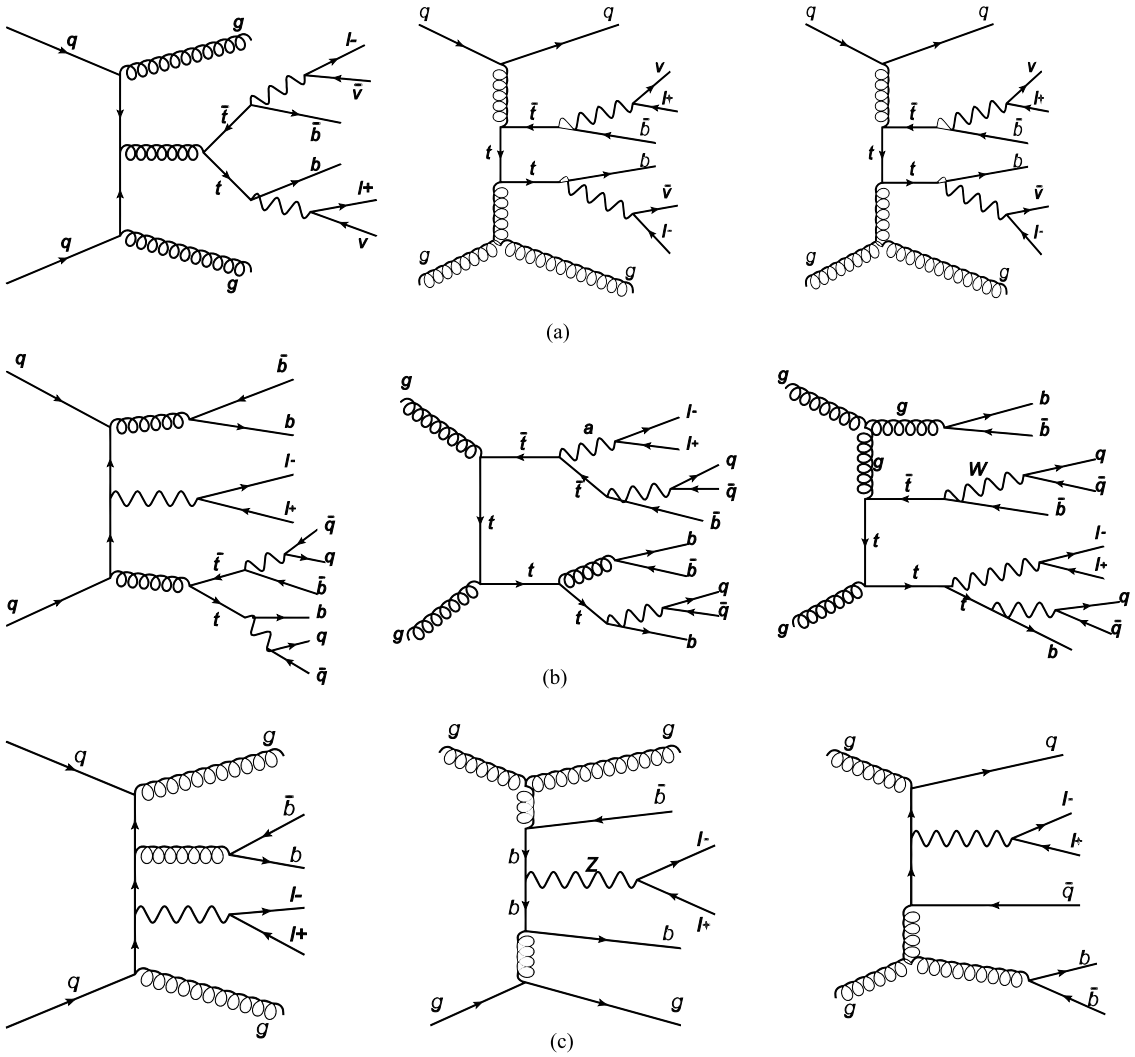

Fig. 5. Feynman diagrams for typical RBs in the case of 2-lepton mode.

• **RB-3:** $\ell^+\ell^- b\bar{b}t\bar{t}$

Processes with a $\ell^+\ell^-$ pair, a $b\bar{b}$ pair and a $t\bar{t}$ pair in the final state. The $t\bar{t}$ pair decay to jets (cf. Fig. 5(b)).

The simulation is similar to the case of the 3-lepton mode, while, in addition, we should take the top quark tagging considering the jet substructure. We make jet clustering using the Cambridge–Aachen (CA) algorithm [26] with radius $R = 1.2$. The jet pruning algorithm [27] with parameters $Z_{\rm cut} = 0.1$ and $RFactor_{\rm cut} = 0.5$ is applied to the CA jets for further suppressing RBs. If the transverse momentum of a pruned CA jet is larger than 350 GeV, we retain it as a boosted jet. The components of the CA jets with $p_T < 350$ GeV are then clustered again by the anti-k_T algorithm with $R = 0.5$. A b-tagging scheme with the same parameters as in Ref. [22] is also performed. We then impose the following cuts:

Cut 1: Requiring the event to contain two isolated opposite-sign leptons and two tagged b jets, i.e.

$$N(\ell^+) = 1,\ N(\ell^-) = 1,\ \ N(b) = 2. \tag{3}$$

Cut 2: Let j_1 be the jet with largest p_T and j_2 be the jet with the second largest p_T. We require

$$p_T(j_i) > 350\ \text{GeV},\ \ |\eta(j_i)| < 2 \tag{4}$$

This can pick up the events containing two boosted jets.

Cut 3: Requiring the mass of the two boosted jets j_1 and j_2 to be in the neighborhood of m_t, i.e.

$$150\ \text{GeV} < M(j_i) < 220\ \text{GeV} \tag{5}$$

This makes j_1 and j_2 two tagged boosted top jets.

Cut 4: Since H is produced by top-quark fusion, its momentum should not be so large. When the two boosted jets are the decay products of an s-channel H, the absolute value of the vector sum of their 3-momenta should be relatively small. So we require

$$|\boldsymbol{p}(j_1) + \boldsymbol{p}(j_2)| < 1\ \text{TeV}. \tag{6}$$

This makes the two boosted top jets coming from H decay.

The cross sections (in fb) of S + IB, IB, and three RBs at the 50 TeV SppC after the cuts are listed in Table 4. We see that after the four cuts, the backgrounds are reduced to the same order of magnitude as S + IB.

Since the two top jets from H decay for $M_H < 800$ GeV can hardly satisfy cut 2, we take the cases of $M_H = 1$ TeV and $M_H = 800$ GeV to plot the invariant mass distributions for an integrated luminosity of 3 ab^{-1} at the 50 TeV SppC in Fig. 6. the resonance peaks can be observed. Note that the resonance peaks in Fig. 6 are not clear enough for precision measurement of M_H. A more sophisticated, while complicated, top tagging algorithm [28,29] may improve the results.

Table 4
Cross sections (in fb) of S + IB, IB and RBs for various values of M_H at the 50 TeV SppC after each cut in the case of 2-lepton mode.

	S + IB				IB	RB-1	RB-2	RB-3
	400 GeV	600 GeV	800 GeV	1 TeV				
Cut 1 & 2	1.05	0.70	0.65	0.62	0.40	34.6	1.79	0.06
Cut 3	0.086	0.061	0.063	0.07	0.036	0.30	0.0096	0.00049
Cut 4	0.032	0.022	0.022	0.026	0.013	0.067	0.0012	0.00011

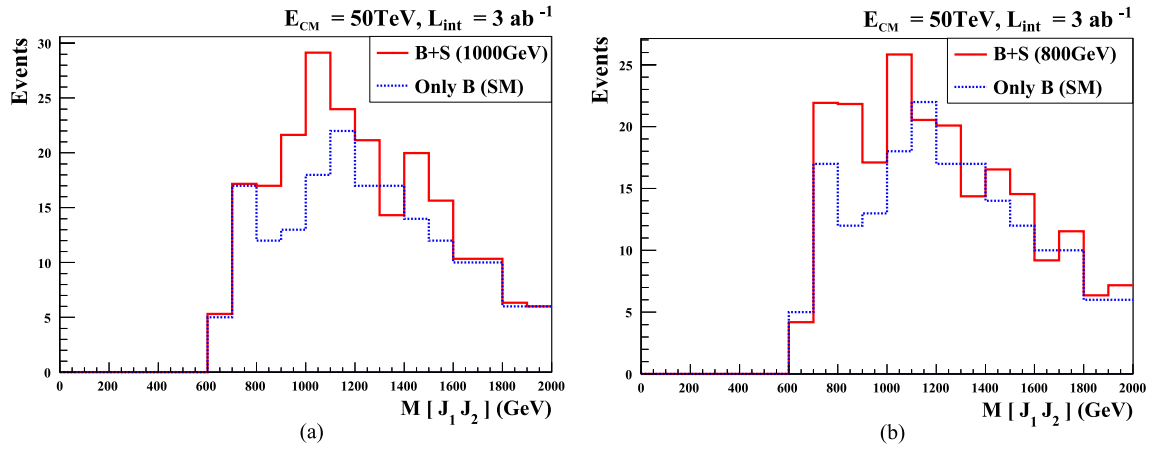

Fig. 6. $M(j_1, j_2)$ distributions (red-solid) for an integrated luminosity of 3 ab^{-1} at the 50 TeV SppC: (a) $M_H = 1$ TeV, (b) $M_H = 800$ GeV. The SM background (blue-dotted) is also plotted for comparison.

3. Summary

In this paper, we have studied the probe of the gauge-phobic heavy Higgs bosons H, usually appear in new physics models, at the 14 TeV LHC and the 50 TeV SppC via the process $pp \to t\bar{t}t\bar{t}$ mainly contributed from gluon fusion. We take the general (model-independent) $Ht\bar{t}$ Yukawa interaction form in Eq. (1).

Our calculation is at the hadron level including simulating the jet formation and top quark tagging (with jet substructure) taking account of the requirement of the detector acceptance. For suppressing the SM background, we take two of the decay modes of the top quarks including leptons, namely the 3-lepton mode and the 2-lepton mode. the former can have negligible SM RBs, and the latter can make the resonance peak of H visible.

In the 3-lepton mode, the needed integrated luminosities for $1\sigma, 3\sigma$ and 5σ deviations from the SM background are shown in Table 3. The case of 5σ for $M_H = 600$ GeV, and the cases of 3σ and 5σ for $M_H \geq 800$ GeV at the LHC require very high luminosities which need the upgraded high luminosity LHC. All other cases can be reached at the present 14 TeV LHC and the SppC. We have further shown that the mass of H can be experimentally determined by measuring the $p_T(b_1)$-distribution at the 50 TeV SppC for an integrated luminosity of 3 ab^{-1} (cf. Figs. 3 and 4).

In the 2-lepton mode, we imposed a series of cuts to suppress the background, and extracted the process that the t and $\bar{t}$ with hadronic decays are from the H decay. The plotted invariant mass distributions $M(j_1, j_2)$ at the 50 TeV SppC for an integrated luminosity of 3 ab^{-1} are shown in Fig. 6 which shows that the resonance peak of H can be observed. But the peak is not clear enough to give a very accurate measurement for M_H. More sophisticated top tagging algorithm [28,29] compared with the simple one used here may help to highlight the resonance peaks.

Acknowledgements

We would like to thank Tsinghua National Laboratory for Information Science and Technology for providing their computing facility. This work is supported by the National Natural Science Foundation of China under the grant numbers 11135003 and 11275102.

References

[1] G. Aad, et al., ATLAS Collaboration, Phys. Lett. B 716 (2012) 1; W. Adam, et al., CMS Collaboration, Phys. Lett. B 716 (2012) 30.
[2] S. Chatrchyan, et al., CMS Collaboration, J. High Energy Phys. 1306 (2013) 81; S.M. Consonni, et al., ATLAS Collaboration, arXiv:1305.3315.
[3] ATLAS Collaboration, ATLAS-CONF-2014-09, 2014.
[4] CMS Collaboration, CMS-PAS-HIG-14-009, 2014.
[5] M. Flechl, on behalf of CMS and ATLAS Collaboration, arXiv:1503.00632.
[6] R. Dashen, H. Neuberger, Phys. Rev. Lett. 50 (1983) 1897.
[7] L. Susskind, Phys. Rev. D 20 (1979) 2619.
[8] G. Degrassi, et al., J. High Energy Phys. 1208 (2012) 098.
[9] G. Aad, et al., ATLAS Collaboration, Phys. Rev. D 89 (2014) 032002.
[10] Yu-Ping Kuang, Hong-Yu Ren, Ling-Hao Xia, Phys. Rev. D 90 (2014) 115002.
[11] P.S. Bhupal Dev, A. Pilaftsis, J. High Energy Phys. 1412 (2014) 024.
[12] G. Bevilacqua, M. Worek, J. High Energy Phys. 1207 (2012) 111.
[13] J. Alwall, M. Herquet, F. Maltoni, O. Mattelaer, T. Stelzer, J. High Energy Phys. 1106 (2011) 128.
[14] A. Alloul, N.D. Christensen, C. Degrande, C. Duhr, B. Fuks, Comput. Phys. Commun. 185 (2014).
[15] D. Stump, J. Huston, J. Pumplin, W.-K. Tung, H.-L. Lai, S. Kuhlmann, J.F. Owens, J. High Energy Phys. 0310 (2003) 046.
[16] T. Sjostrand, S. Mrenna, P. Skands, J. High Energy Phys. 0605 (2006) 026.
[17] J. Favereau, C. Delaere, P. Demin, A. Giammanco, V. Lemaitre, A. Mertens, M. Selvaggi, J. High Energy Phys. 1402 (2014) 057.
[18] M. Cacciari, G.P. Salam, G. Soyez, Eur. Phys. J. C 72 (2012) 1896.
[19] S. Chatrchyan, et al., CMS Collaboration, J. Instrum. 3 (2008) S08004.
[20] CMS Collaboration, CERN-PH-EP-2014-222, 2014.
[21] Daniela Paredes, CERN-THESIS-2013-202.
[22] A. Avetisyan, et al., arXiv:1308.1636, 2013.
[23] Note that the width of the GPHB is not large, e.g., even for an $M_H = 1$ TeV GPHB, its width is just 40 GeV. Thus in the vicinity of M_H, the contribution from the interference term is much smaller than the total resonance contribution. So this definition of σ_S essentially reflects the property of the signal.
[24] A. Abdesselam, et al., Eur. Phys. J. C 71 (2011) 1661.

[25] A. Altheimer, et al., J. Phys. G 39 (2012) 063001.
[26] Y.L. Dokshitzer, G.D. Leder, S. Moretti, B.R. Webber, J. High Energy Phys. 9708 (1997) 001.
[27] S.D. Ellis, C.K. Vermilion, J.R. Walsh, Phys. Rev. D 80 (2009) 051501;
S.D. Ellis, C.K. Vermilion, J.R. Walsh, Phys. Rev. D 81 (2010) 094023.
[28] D.E. Kaplan, K. Rehermann, M.D. Schwartz, B. Tweedie, Phys. Rev. Lett. 101 (2008) 142001.
[29] T. Plehn, M. Spannowsky, J. Phys. G 39 (2012) 083001.